Synthesis of Nitrogen-Doped Carbon Nanostructures by the Reactions of Small Molecule Carbon Halides with Sodium Azide

Changzheng Wu, Qixun Guo, Ping Yin, Tanwei Li, Qing Yang, and Yi Xie*

Nanomaterials and Nano-chemistry, Hefei National Laboratory for Physical Sciences at Microscale, University of Science & Technology of China, Hefei, Anhui 230026, China

Received: October 1, 2004; In Final Form: November 11, 2004

Nitrogen-doped carbon nanostructures including particles, whiskers, square frameworks, lamellar layers, hollow spheres, and tubular structures have been successfully synthesized by designed direct chemical reactions of small molecule carbon halides (such as CCl_4, C_2Cl_6) and nitridation reagent NaN_3 in the absence of any templates and catalysts. The N/C ratios of the as-prepared CN_x nanostructures (0.01∼0.33) are strongly and systematically related to the reaction temperatures and the choice of carbon sources, as well as the presence or absence of the solvent. The Raman spectra indicate that the approaching graphitization process has occurred as the reaction temperature increases. The possible reaction mechanisms for the formation of the hollow structures are tentatively discussed according to the experimental results. This strategy provides an alternative route to synthesize nitrogen-doped carbon nanostructures and is expected to open up a new route for the synthesis of carbon nitrides.

1. Introduction

Doping carbon nanostructures with nitrogen atoms has sparked a worldwide interest because the incorporated N can enhance the mechanical, conducting, field emission, energy storage, and electron transport properties of the nanostructures.[1] The stimulus for this study also stems from the theoretical predictions of the hypothetical metallic CN nanotubes[2] and covalently bonded β-C_3N_4[3], both possessing an unmatched hardness. Up to now, considerable efforts have been made to study the preparation and growth mechanism of the carbon nitrides (CN_x). The most extensively used methods to fabricate N-substituted carbon structures are chemical vapor deposition (CVD),[4] most of which relied on catalytic pyrolysis of C or CN gas-phase precursors under N-rich atmosphere and were usually carried out under relatively high temperatures. In this case, whether the N-rich solid precursors are utilized in the pyrolysis process or not, the highest N doping level reported so far is only to <13%,[5] implying difficulty in the formation of a C−N bond; the incorporation of nitrogen into carbon is not easily undertaken because of the greater thermodynamic stability of carbon and separate nitrogen molecules at the high reaction temperature.[6] To explore other alternatives, some precursors containing ═C−N units linked by sp^2 carbons may be catalytically converted to sp^2 CN_x structures with or without solvents. In most of the reported reactions, cyanuric chloride ($C_3N_3Cl_3$), which contains three ═C−N units, is widely chosen as the building blocks to synthesize carbon nitrides with hollow spheres,[7] nanotubes,[8] particles,[9] and so on. On the account of its toxic properties, it is inconvenient to employ the cyanuric chloride as the initial reagent. Since the small molecule compounds of carbon halides may serve as the carbon source for the carbon nanostructure growth elsewhere,[10] we believed that CN_x could be directly synthesized under appropriate conditions using small molecule carbon halides as precursors. Although the attempt has been made to study the reaction of carbon halides hexachlorobutadiene (C_4Cl_6) with NaN_3 very recently, the nitrogen contents seemed to be ignored there.[11] Thus, the development of a new methodology for preparation of CN_x nanostructures where carbon halides were used as carbon source would be significant for the further investigation in this area.

In this manuscript, we have designed several chemical reaction routes to prepare CN_x (0.01∼0.33) nanostructures using small molecule carbon halides (such as CCl_4, C_2Cl_6) as the carbon source and sodium azide (NaN_3) as the nitrogen source in the solution or solvent-free conditions. Some artistic morphologies of nitrogen-doped carbon nanostructures such as particles, whiskers, square frameworks, lamellar layers, hollow spheres, and tubular structures have been obtained. To our best knowledge, this is the first example for the high-yield selected-control preparation of nitrogen-doped hollow spheres, whiskers, and tubular structures without the use of any templates and catalysts. Moreover, the nitrogen contents of these nitrogen-doped carbon nanostructures have a controllable manner by adjusting the different reaction parameters (reaction temperatures, with or without solvents, carbon sources, etc.).

2. Experimental Section

To prepare nitrogen-doped carbon nanostructures, CCl_4 (1.54 g, 10 mmol) and NaN_3 (2.60 g, 40 mmol) were loaded into a 60-mL stainless steel autoclave, which was then filled with benzene (pretreated by metal Na for 30 min to remove H_2O) up to 80% of the total volume. All the above manipulations were performed in a glovebox with flowing nitrogen gas. The autoclave was sealed, heated to 220 °C (or 230 °C, 250 °C, 300 °C, 350 °C, 450 °C) for 8 h. The product was filtered and washed with dilute HCl, distilled water, and acetone to remove NaCl and other impurities. Finally, the as-synthesized products were dried under vacuum at 60 °C for 3 h. For comparison, keeping the other experimental parameters constant, studies of various reaction temperatures (350 °C, 450 °C, 550 °C, and

* Author to whom correspondence should be addressed. Tel: 86-551-3603987; fax: 86-551-3603987; e-mail: yxielab@ustc.edu.cn.

10.1021/jp045530m CCC: $30.25
Published on Web 01/22/2005

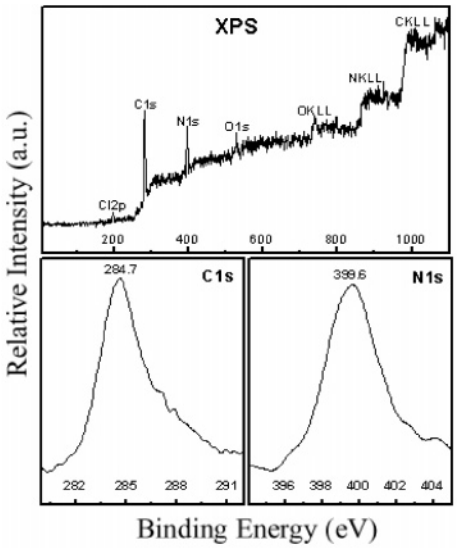

Figure 1. Typical XPS spectra of the sample obtained by the reaction of CCl_4 and NaN_3 at 220 °C.

650 °C) without the solvent were also carried out. When C_2Cl_6 (1.19 g, 5 mmol) substituted CCl_4 in this system, different temperatures (220 °C, 300 °C, 350 °C, 450 °C) and different conditions (the presence and absence of benzene solvent) were also studied. The whole reaction process can be formulated as follows:

$$C_nCl_{2n+2} + NaN_3 \rightarrow \text{nitrogen-doped carbon nanostructures} + NaCl + N_2 + \text{byproducts} \quad n = 1, 2$$

The presence of NaCl has been confirmed by the XRD pattern of the brown-black (or black) products before washing by dilute HCl, distilled water, and acetone in our experiments (not shown here). In addition, there are no designed nitrogen-doped carbon products obtained in the absence of benzene both for CCl_4-NaN_3 and $C_2Cl_6-NaN_3$ systems when the reaction temperature is lower than 300 °C, indicating that the benzene solvent promotes the reaction between carbon halides and NaN_3 at a relatively low temperature of <300 °C.

X-ray photoelectron spectroscopy (XPS) measurements were performed on a VGESCALAB MKII X-ray photoelectron spectrometer with an exciting source of Mg Kα = 1253.6 eV. IR absorption spectra were performed with a Nicolet FT-IR-170SX spectrometer in the range of 500∼4000 cm^{-1} at room temperature, in transmission mode in a KBr pellet. The transmission electron microscopy (TEM) images were performed with a Hitachi Model H-800 instrument with a tungsten filament, using an accelerating voltage of 200 kV. Raman spectra were recorded at room temperature with a LABRAM-HR Confocal Laser MicroRaman Spectrometer. Photoluminescence spectroscopy (PL) was carried out on a Shimadzu RF-5301PC spectrofluorophotometer with a Xe lamp at room temperature.

3. Results and Discussion

3.1 Composition of the Products. The evidence for purity and composition of the sample is obtained by XPS measurements. Figure 1 shows the typical XPS spectra of the product obtained by the reaction of CCl_4 and NaN_3 at 220 °C in the benzene-thermal system. The survey spectrum indicates the presence of C, N, and O impurity from absorbed gaseous molecules and the absence of any impurity such as Cl or Na. High-resolution spectra are also recorded in the C 1s and N 1s regions. The peak cores at 284.8 and 399.6 eV correspond to C1s and N 1s, respectively, which were close to the reported binding energies.[12] Furthermore, the C1s peak showing an asymmetry in the right part can be attributed to C−N bonds and the peak shifting slightly to higher binding energies suggests the combination between C and N.[13] By measuring peak areas of N and C cores, the ratio of N/C is calculated to be 0.33.

TABLE 1: The N/C Ratios of Various Nitrogen-Doped Nanostructures Obtained by Different Carbon Sources and Different Reaction Temperatures

group number	reactants	reaction temperature	N/C ratios
1	CCl_4, NaN_3 (in benzene)	<200 °C	no products
		220 °C	0.33
		230 °C	0.28
		250 °C	0.20
		300 °C	0.09
		350 °C	0.06
		450 °C	0.01
		<300 °C	no products
2	CCl_4, NaN_3 (solvent-free)	350 °C	0.09
		450 °C	0.07
		550 °C	0.02
		650 °C	0.01
		220 °C	0.18
3	C_2Cl_6, NaN_3 (in benzene)	300 °C	0.07
		350 °C	0.04
		450 °C	0.01
4	C_2Cl_6, NaN_3 (solvent-free)	350 °C	0.04
		450 °C	0.01

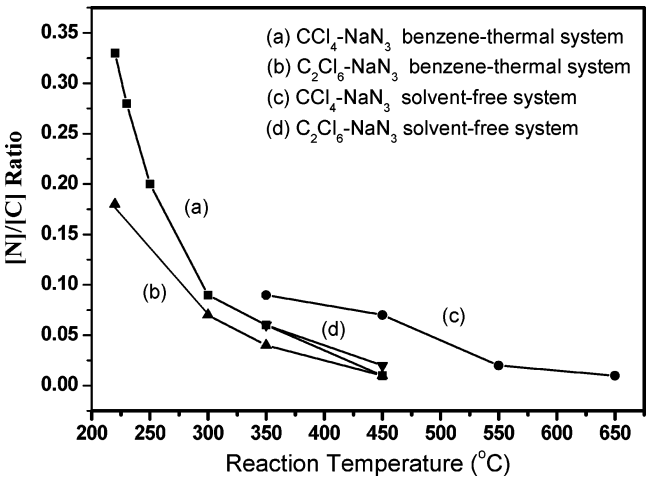

Figure 2. Curve diagram for the N/C ratio as a function of the reaction temperature in the various systems.

In addition, the samples obtained by different reaction conditions (such as different carbon sources, with or without solvent, different temperatures, etc.) were also measured by XPS analysis. All the XPS analysis results are summarized in Table 1 and the corresponding curve diagram for the N/C ratio as a function of the reaction temperature is shown in Figure 2, from which there are some features that should be noted as follows:

(i) All the curves involved in Figure 2 are monotone decreasing in the concerning reaction temperature scale, indicating that by keeping other reaction parameters constant, the N/C ratio decreases as the reaction temperature increases independent of the presence of the benzene solvent. The curves for both CCl_4-NaN_3 system and $C_2Cl_6-NaN_3$ system in the solvent-assisted systems in Figure 2 show the sharp decline in the range from 220 to 300 °C, that is to say, the nitrogen contents sharply decrease in this temperature range. This fact confirms that the incorporation of nitrogen into carbon seems to be not easily

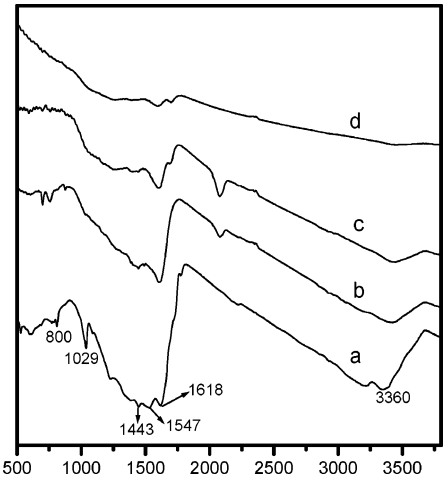

Figure 3. FT-IR spectra of nitrogen-doped carbon nanostructures obtained by the reaction between CCl_4 and NaN_3 with the presence of benzene solvent at different reaction temperatures (a) 220 °C, [N]/[C] = 0.33; (b) 300 °C, [N]/[C] = 0.09; (c) 350 °C, [N]/[C] = 0.06; (d) 450 °C, [N]/[C] = 0.01.

undertaken at the higher reaction temperatures, leading to the decrease of nitrogen contents.

(ii) Keeping other conditions constant, when the carbon atom number in the molecules of carbon sources increases (from CCl_4 to C_2Cl_6, etc.), the N/C ratios in the products clearly decrease. The corresponding curve for the CCl_4-NaN_3 benzene-thermal system (Figure 2a) is always on the upward side of that for $C_2Cl_6-NaN_3$ benzene-thermal system (Figure 2b), suggesting that the nitrogen content of products obtained by the reaction between CCl_4 and NaN_3 is higher than that of the products by the reaction between C_2Cl_6 and NaN_3 in the benzene solvent conditions at the certain temperature.

(iii) The N/C ratios of the products obtained in the absence of any solvents are usually higher than that of the products obtained by the solvent-assisted reaction (for CCl_4-NaN_3 system, at 350 °C: 0.09 in solvent-free system, >0.06 in benzene-thermal system; at 450 °C: 0.07 in solvent-free system, >0.01 in benzene-thermal system; for $C_2Cl_6-NaN_3$ system: at 350 °C: 0.06 in solvent-free system, >0.04 in benzene-thermal system; at 450 °C: 0.02 in solvent-free system, >0.01 in benzene-thermal system). This fact indicates that the presence of solvent indeed influences the nitrogen contents to some extend.

The typical IR spectra further imply the existence of the substance CN_x and show the fact that the higher the temperature is, the lower N content is. Here, the products obtained by the reaction of CCl_4 and NaN_3 in benzene-thermal system in the temperature range of 220∼450 °C are taken as an example. The IR strong absorption at 1618 cm^{-1} is due to the CC sp^2 phase.[14] The N introduction is distinctly shown in Figure 3a: the absorption bands centered at 1029, 1443, and 1547 cm^{-1} can be attributed to N−N,[15] N═N,[16] and C═N,[8] respectively. The broad band at about 3360 cm^{-1} is supposed to be N−H,[17] and the peak at 800 cm^{-1} belongs to s-triazine ring modes.[8] As is known, a large dynamic charge for π states which results from the small energy gap of the π states and the conjugated π bonding of sp^2 sites contributes to IR intensity.[14] The introduction of nitrogen induces an increase and clustering of the sp^2 phase and promotes charge fluxes within the molecule and thus higher IR absorption, shown in the four spectra in Figure 3. In this case, the spectra of the as-obtained products obtained at 220, 300, 350, and 450 °C are summarized in Figure 3, from which one can see that compared with the spectrum of Figure 3a, the intensity of IR absorption in Figure 3b−d turns weaker gradually with the increasing of reaction temperatures. In addition, the peaks at 1029 cm^{-1}, 1443 cm^{-1}, and 3360 cm^{-1} disappear gradually, and even the band at 1547 cm^{-1} gets to be considerably weak. It is clear that it is the decrease of N content that leads to the weaken IR absorption.

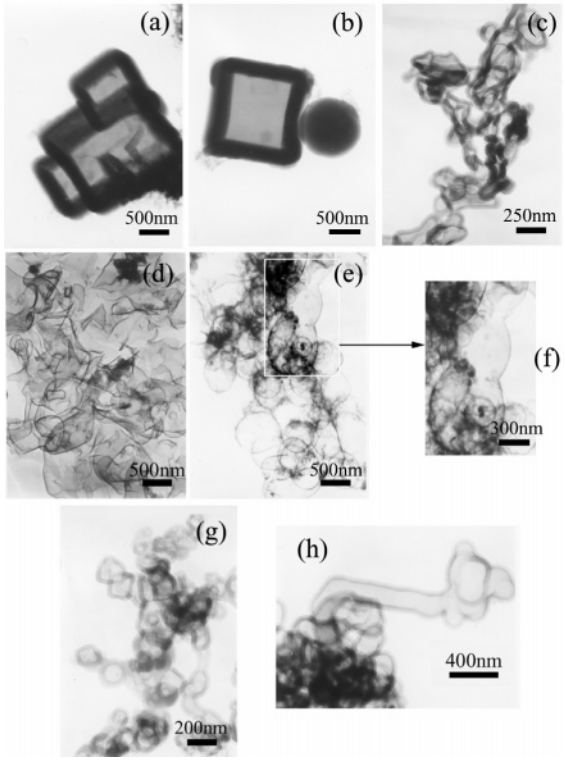

Figure 4. TEM images of the products for the as-prepared CN_x obtained by the reaction between CCl_4 and NaN_3 in benzene-thermal systems at different reaction temperature: 220 °C, some particles and square frameworks (a−b); 300 °C, some quasi-hollow spheres (c) and flakes (d); 350 °C, some hollow spheres (e) and the enlarged region show the coexistence of the segmental vessels (f); 450 °C, hollow spheres (g) and a typical vessel (h).

3.2 Morphologies of the Products. *3.2.1 For CCl_4-NaN_3 System.* Figure 4 shows the TEM evolution of the products obtained by the direct reactions between CCl_4 and NaN_3 from 220 to 450 °C in benzene-thermal system. The nitrogen-doped carbon nanostructures obtained at 220 °C mainly consisted of particles (70%), with coexistence of minor square frameworks (20%, shown in Figure 4a and b). It is evident that the boundary of the square frameworks is quite well defined. The external diameter of the square frameworks is 600∼900 nm and the thickness of the wall is about 80∼200 nm. When the reaction temperature was elevated to 300 °C, there were no solid morphologies anymore and the representative TEM images (Figure 4c and d) of the as-obtained products showed that both quasi-hollow spheres (60%) and some flakes (20%) could be found in the final products. At the temperature of 350 °C, the morphologies appear to be the hollow spheres (80%) mostly with the external diameter of 300∼800 nm and the thickness of the wall is less than 20 nm (Figure 4e). Interestingly, by careful observation on these hollow structures, there exists some segmental vessels (5%) with the reminiscence of hollow spherical morphology (Figure 4f), suggesting the probable relation between the hollow spheres and the vessel structures. Additionally, the sample prepared at 450 °C consists of 70∼75% hollow spheres (Figure 4g) and 10∼15% vessels (Figure 4h). Figure 4h shows the typical vessels whose external diameter and length is 200 nm and 3000 nm, respectively. These vessels

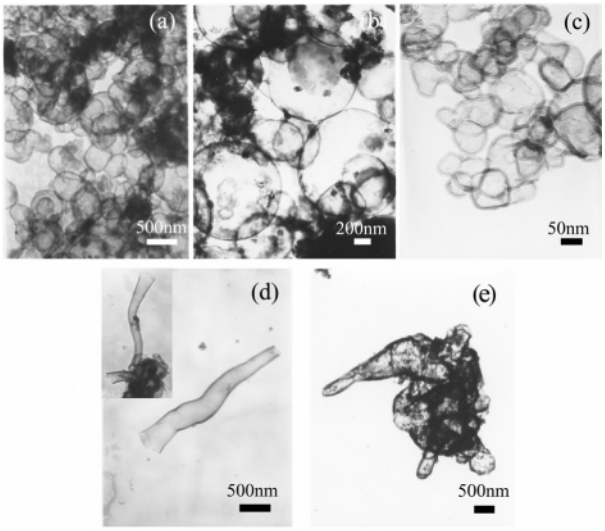

Figure 5. TEM images of the products for the as-prepared CN_x obtained by the reaction between CCl_4 and NaN_3 in solvent-free systems at different reaction temperatures: (a) 350 °C, hollow spheres. (b−d) 450 °C, hollow spheres with different diameters and some vessels. (e) 550 °C, some collapsing hollow structures.

clearly show smooth morphology although the reminiscence of hollow spherical morphology at the one tip of the vessel is found in Figure 4h.

In the solvent-free system, at lower than 330 °C, no products were obtained after the water and hydrochloric acid treatment. At 350 °C, it can be seen that the sample consists of hollow spheres 40∼1100 nm (80%) in diameter as shown in Figure 5a. In this case, there are no tubular morphologies found in the final products. As for the products obtained at 450 °C, the hollow sphere size distribution is similar to that obtained at 350 °C and the size of these hollow spheres ranges from 40 nm to several micrometers remaining the thickness of the shell less than 20 nm (Figure 5b and c). However, a more detailed investigation of the as-prepared products by TEM reveals that besides the hollow spheres (60%), some vessels with open ends (15%) appear, which are different from that of product obtained at the lower temperature of 350 °C, where there are no tubular morphologies. From Figure 5d, we can observe that the vessel has two open ends with the length of 2400 nm. The inner diameter of the vessel is 150 nm and the outer diameter is 170 nm on average. The shell thickness of the hollow spheres is similar to that of the vessels. However, when the temperature was elevated to 550 °C, these hollow structures seem to be collapsing and the main morphology is the particles (70%). Figure 5e shows the typical morphology of collapsing vessels. When the reaction temperature is higher than 600 °C, there are only particles (80%) obtained, rather than the hollow structures as described above.

3.2.2 C_2Cl_6−NaN_3 Systems. TEM images of as-obtained nitrogen-doped carbon structures obtained by using C_2Cl_6 as carbon source in the solution conditions are shown in Figure 6. At the temperature of 220 °C, it can be seen that the product in this case is uniform whiskers (85%) with the width of 400∼600 nm and the length up to several micrometers (Figure 6a). Figure 6b is the typical nitrogen-doped solid whiskers. However, at 300 °C the morphology of the products is some flakes (30%, shown in Figure 6c) and some vessels (40%, shown in Figure 6d−f), rather than the solid whiskers obtained at the lower temperature of 220 °C. Both sides of these tubular structures reveal obvious step edges, which cause the rough surface and nonuniform diameter along the vessels. A more detailed

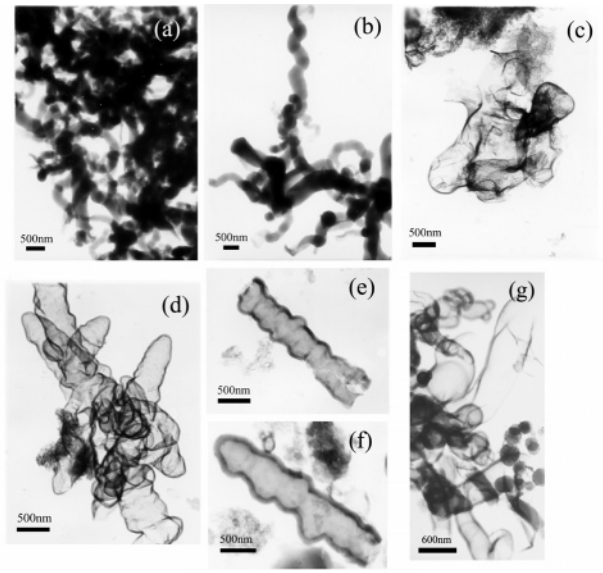

Figure 6. TEM images of the products for the as-prepared CN_x obtained by the reaction between C_2Cl_6 and NaN_3 in benzene-thermal systems at different reaction temperatures: 220 °C, some whiskers (a) and the enlarged region of the whiskers (b); 300 °C, some flakes (c) with coexistence of some vessels (d) and the typical vessels with one open end (f) and two open ends (e); 450 °C, some vessels (g).

investigation of as-prepared products reveals that there are two kinds of nitrogen-doped carbon vessels, a kind of vessel with open ends (Figure 6e) and another with closed ends (Figure 6f). As for the product obtained at the higher temperature of 450 °C (Figure 6g), one can find that the shell of these vessels turned to be smooth and there is not any roughness in the sides at all, although the yield of the products seems to be not high (30%).

For the solvent-free systems at 350 °C and 450 °C, the morphology is similar to that of the products using CCl_4 as the carbon source in the absence of benzene. In this case, the as-prepared product shows that there are hollow spheres (60%, Figure 7a) at 350 °C. However, at 450 °C, besides the hollow spheres (55%, Figure 7b), tubular structures (10%, Figure 7b), and some segmented vessels (5%, Figure 7c) can also be seen, further confirming that the higher temperatures favor the appearance of tubular structures.

The schematic diagram of the morphology evolution both for the CCl_4−NaN_3 and C_2Cl_6−NaN_3 systems in the presence or absence of benzene as a solvent is shown in Figure 8 for clarity.

3.3 Raman Spectra: in the CCl_4−NaN_3 System in Benzene. The technique of Raman spectroscopy is sensitive to the grain size in nanometric and amorphous structures for the cross-linking of graphitic planes.[18] To study the microstructure evolution of different temperatures (or different N/C ratios), the samples obtained by the reaction of CCl_4 and NaN_3 in benzene-thermal system are taken as an example (Figure 9). No arbitrary scaling factors were introduced, though successive curves (Figure 9a) are translated downward for clarity. The band between 1000 and 2000 cm^{-1} corresponds to the first-order Raman spectrum of disordered sp^2 carbon. With increasing nitrogen content, these bands become stronger, which means that Raman active G and D bands and others become more active when large amounts of nitrogen are present in the products. Kaufman et al.[19] conclude that nitrogen substitution is responsible for the symmetry breaking of the E_{2g} mode and the intensity of the G and D bands. Thus, the intensity of the sp^2 line is sensitive to nitrogen concentration and the 1350−

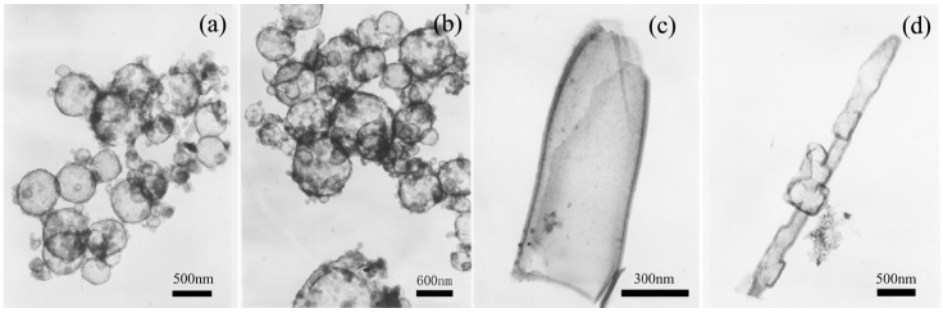

Figure 7. Typical TEM images of the products for the as-prepared CN_x obtained by the reaction between C_2Cl_6 and NaN_3 in solvent-free systems at the temperature 350 °C, some hollow spheres (a); 450 °C, some hollow spheres (b), a tubular structure (c), a segmented vessel (d).

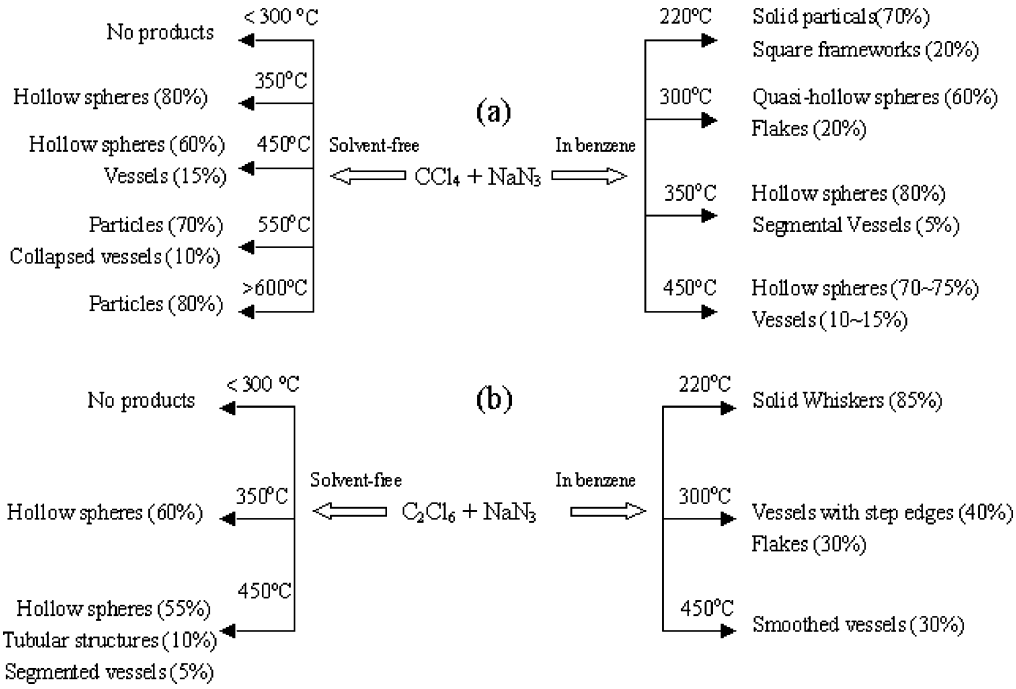

Figure 8. Schematic diagram of the morphology evolution for the CCl_4-NaN_3 system (a) and $C_2Cl_6-NaN_3$ system (b) in the presence or absence of benzene as a solvent (the percentage as shown above is the morphology proportion based on the TEM photo).

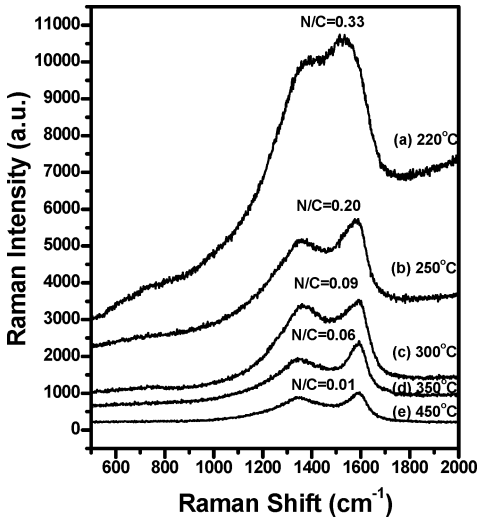

Figure 9. Raman spectra for the samples obtained by the reaction of CCl_4 and NaN_3 in benzene-thermal system.

1650 cm^{-1} band feature is mostly due to the difference in nitrogen concentration.

To obtain information about the microstructure of the products, the first-order band of the carbon stretching mode between 1000 and 2000 cm^{-1} was fitted with a linear background and two Gaussian distributions, labeled "G" (graphite) and "D" (disorder).[20] This analysis is similar to what is done in the study of amorphous carbon.[21] The results of the fitting analysis are shown in Figure 10. First, all the positions of the G peak (from 1563.8∼1590.6 cm^{-1}) in panel a are close to the crystalline graphite value (1580 cm^{-1}). With increasing nitrogen content, the G band shifts toward lower frequencies, indicating a distortion of graphitic network.[22] Second, Figure 10b shows the relative intensity I_D/I_G, which is a usual measurement of the graphitic ordering. In this case, the incorporation of nitrogen induces the increase of the I_D/I_G ratio, indicating a distortion of the graphitic network and a decrease of graphitic domain size with increasing nitrogen contents. In our experiments, N/C ratios decrease as the reaction temperature increases independent of the presence of the benzene solvent, which leads to the decrease of the I_D/I_G ratio. The decrease of I_D/I_G indicates that the number of sp^2 bonded carbon atoms without dangling bonds have increased and the low ratio I_D/I_G is characteristic of a graphite lattice with perfect two-dimensional order in the basal plane.[23] That is to say, as for the as-obtained CN_x products, it indicates that the approaching graphitization process has occurred as the reaction temperature increases.

3.4 Possible Mechanism for As-Obtained CN_x Morphologies. On the basis of the above results, although the conformation and bonding topology of the as-obtained CN_x materials are

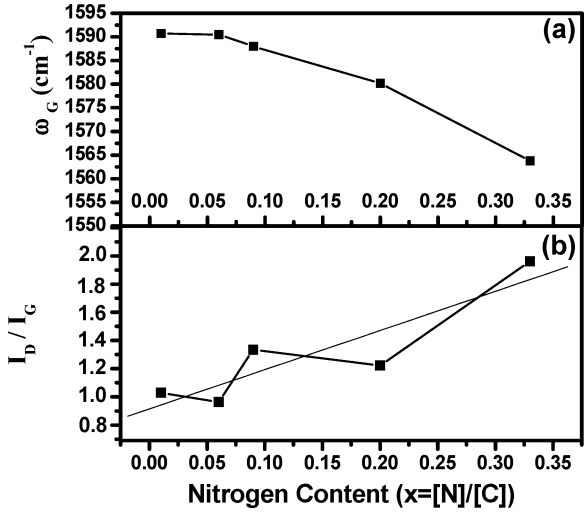

Figure 10. Fitting parameters of the Raman spectra as a function of the nitrogen fraction: position of the G peak (a) and relative intensity of the D and G peaks (b). The straight line in b is achieved by performing a linear fit on the data point in b.

not yet fully understood, it is reasonable to believe that these CN_x materials consist of a large carbon graphite cluster randomly substituted by nitrogen.[24] Thus, the appearance of these artistic structures such as vessels with step-edge shells or smooth shells, hollow spheres with different sizes, and different nitrogen contents are basically determined by the N-substituted graphitelike layer structures. Under certain conditions, as for graphitelike materials, the growth reaction rate along the certain axis is much lower than that along any other axis which will lead to the formation of the lamellar structures.[25] Furthermore, the interaction of the lamellar interlayers could be diminished from the edges and then the rolling process could proceed. The sealed system with high temperature and pressure is also beneficial for the rolling of the sheets, which is similar to the fact that graphite and other fullerenic material layers (such as BN, replacement of pairs of carbon atoms by the isoelectronic B−N pairs in the hexagonal network of graphite leads to a whole array of 2-D phases) curled with the assistance of various driving forces. Heidenreich et al. have noted that severe bending of graphite sheets commonly occurs at a high temperature,[26] and Ugarte et al. reported that curling graphitic networks have been observed under electron beam irradiation.[27] In addition, our group has recently reported the appearance of BN vessels, hollow spheres, onions, and peanuts by a synergic nitrogen source route,[28] in which the high pressure coming from NH_3 and HCl provides a kind of metastable growth condition, leading to the rolling of the lamellar h-BN structures to form hollow structures. All these studies give us the inspiration that the possibility of the similar rolling process for the lamellar CN_x structures existed in the sealed system with high pressure and temperature. The coexistence of hollow spheres or vessels and the rolling lamellar structures (shown in Figure 4c−d and Figure 6c, respectively) is the direct evidence for the rolling process and suggests the link between the lamellar structure intermediates and the hollow structures (spheres, vessels), corresponding well to the rolling process mechanism. As for the reaction conditions in this work, the high pressure coming from the vapor pressure of the solvent or N_2 produced in the reaction process might also provide a certain kind of metastable growth condition. As is well known for graphite and graphitelike materials, the reactivity of atoms (carbon or nitrogen) in edge site positions is far greater than those within basal plane positions.[29] Therefore, the CN_x layers are tentative to join the edges and then close up to form the corresponding hollow structures. Here, an alternative mechanism for the annihilation of the peripheral dangling bonds may be raised, which leads to the formation of hollow nanostructures. For this process to take place, sufficient thermal energy and pressure are required to overcome the activation barriers associated with the bending of the layers (elastic strain energy).[26] In this case, vessels with step-edge shells or smooth shells, hollow spheres with different sizes, and different nitrogen contents are fabricated.

Now, we concentrate on the possible formation mechanism of vessels in the CCl_4-NaN_3 systems in the presence and absence of benzene solvent. From the experimental results, one can see that the high temperature favors the formation of vessels to some extent and the low temperature only leads to hollow spheres. Careful observation on the products obtained at 350 °C in solvent system shows that there exist some segmental vessels with the reminiscence of hollow sphere morphology (Figure 4e and f). Another interesting phenomenon is that in the TEM image of Figure 4h, there are some separated cavities, whose shells have spherical morphology at one tip of the vessels. This fact indicates that the reaction temperatures are vital for control of the nanostructures, perhaps because hollow spheres have less surface strain and need less energy to form.[30] Thus, at higher temperatures, the restructing of these nitrogen-doped carbon materials is enabled by bond breaking and reforming.[31] Some hollow spheres become joined to each other to form aligned hollow spheres and their shells form twins (so-called segmental vessels, Figure 4e and f), and then they form the well-defined vessels with the assistance of high temperature.

It is apparent that the reaction temperature has a prominent effect on the morphology of CN_x both in the CCl_4-NaN_3 and $C_2Cl_6-NaN_3$ systems as well as the nitrogen content. First, both the CCl_4-NaN_3 and $C_2Cl_6-NaN_3$ systems in benzene-thermal conditions posess a similar morphology evolution from the solid structures, curling sheets, to hollow structures as the reaction temperature increases. At the relative low temperature of 220 °C, there are only solid particles (Figure 4a and b) and solid whiskers (Figure 6a and b) obtained in the presence of benzene as a solvent for the CCl_4-NaN_3 and $C_2Cl_6-NaN_3$ systems, respectively. The curling flakes begin to appear at the elevated temperature of 300 °C (Figure 4c and d and Figure 6c) and then at the hollow structures obtained at the further higher temperatures, indicating the high temperature is beneficial for the formation and curling of the lamellar structures. Second, on one hand, as for the CCl_4-NaN_3 benzene-thermal system, the size of hollow spheres obtained at 450 °C (Figure 4g) is smaller and more uniform than that obtained at 350 °C (Figure 4e). However, in the corresponding solvent-free system, the size distribution of hollow spheres seems to be independent of the temperature range of 350∼450 °C as shown in Figure 5a−c except that tubular morphology is found at the higher temperature of 450 °C, whereas only spherical morphology can be found at 350 °C. On the other hand, as for the $C_2Cl_6-NaN_3$ benzene-thermal system, the contrast between the TEM images in Figure 6d−f (prepared at 300 °C) and those in Figure 6g (prepared at 450 °C) clearly reveals that the vessels show obvious step-edge shells at 300 °C, while their shells turned to be more smooth at the elevated temperature of 450 °C. However, for the $C_2Cl_6-NaN_3$ nonsolvent system, the phenomenon is similar to that of the CCl_4-NaN_3 nonsolvent system: the size distribution at 450 °C is similar to that of 350 °C, whereas the vessels appeared at the higher temperature of 450 °C. Third, when the reaction temperature is up to 550 °C in the CCl_4-

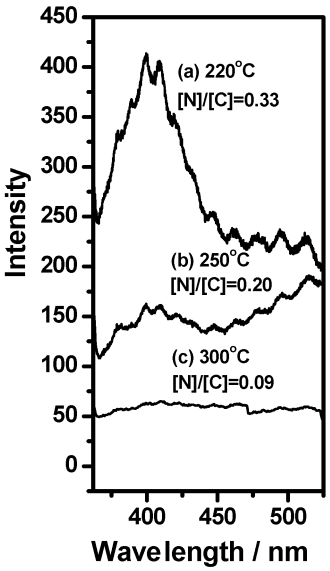

Figure 11. The PL spectra of the as-prepared samples by the reaction of CCl_4 and NaN_3 in benzene-thermal system at the temperature of 220 °C ([N]/[C] = 0.33) (a); 250 °C ([N]/[C] = 0.20) (b); and 300 °C ([N]/[C] = 0.09) (c).

NaN_3 solvent-free system, the hollow structures seem to collapse (Figure 5e), and then only some particles are obtained at the elevated temperature of 650 °C.

In the $C_2Cl_6-NaN_3$ benzene-thermal system, the products favorably possess one-dimensional morphology (whiskers, vessels), which is different from the morphology of the particles, square frameworks, hollow spheres, and so forth obtained in the corresponding CCl_4-NaN_3 benzene-thermal conditions. However, in the solvent-free conditions, the main morphology is hollow spheres for the $C_2Cl_6-NaN_3$ system (Figure 7), which is similar to that of the products using CCl_4 as the carbon source keeping other reaction parameters constant (Figure 5). The reason that the drastic difference is displayed is not fully understood and requires more systematic investigations.

3.5 PL Spectra of CCl_4-NaN_3 Benzene-Thermal System. The typical photoluminescence spectrum of the synthesized CN_x obtained by the reaction of CCl_4 and NaN_3 in benzene-thermal systems shows a broad peak around 400 nm (Figure 11a), which is close to the band gap emission.[32] The decrease of PL intensity is shown in Figure 11b and c as the nitrogen content decreases; it can be seen that there is only a feeble peak in Figure 11b, while no obvious peak can be found as shown in Figure 11c, as well as that of the products of [N]/[C] $\leq$ 0.09 (not shown here). Thus, the intensity of the PL line is sensitive to nitrogen concentration and the intensity feature is mostly due to differences in nitrogen concentration.

4. Conclusions

In summary, we have described a small carbon halides molecule (such as CCl_4 and C_2Cl_6) route to growth of artistic nitrogen-doped carbon nanostructures with the artistic morphologies of nitrogen-doped carbon nanostructures such as particles, whiskers, square frameworks, lamellar layers, hollow spheres, smooth-shell vessels, and vessels with step edges in which the nitrogen contents can be controlled by adjusting different reaction parameters (temperature, solvent, carbon source, etc.). It is apparent that the reaction temperature, solvent, and different carbon sources have a prominent effect on the morphology of CN_x both in the CCl_4-NaN_3 system and the $C_2Cl_6-NaN_3$ system. Moreover, the Raman spectra indicate that the approaching graphitization process has occurred as the reaction temperature increases and the graphitic lamellar structures of CN_x seem to be responsible for the formation of the as-prepared hollow structures in the present work, which is similar to the well-known growth manner of graphite and graphitelike materials. These nitrogen-doped carbon nanostructures obtained from our experiment, especially for the hollow structures, have potential applications similar to their all-carbon counterparts, which have been utilized as hard coatings, lithium intercalation electrodes, metal catalyst supports, and hydrogen storage materials.[33] However, more work is required to exactly understand the growth mechanism of these artistic morphologies.

Acknowledgment. This work was supported by National Natural Science Foundation of China, Chinese Ministry of Education, and Chinese Academy of Sciences. The authors also thank Dr. Shuangzheng Lin for helpful discussion for the formation mechanism.

Supporting Information Available: Fitting parameter process of Raman Spectra for the CCl_4-NaN_3 benzene-thermal system at different temperatures is shown in Supplementary Figure 1. This material is available free of charge via the Internet at http://pubs.acs.org.

References and Notes

(1) (a) Terrones, M.; Ajayan, P. M.; Banhart, F.; Blase, X.; D.; Carroll, L.; Charlier, J. C.; Czerw, R.; Foley, B.; Grobert, N.; Kamalakaran, R.; KohlerRedlich, P.; Ruhle, M.; Seeger, T.; Terrones, H. *Appl. Phys. A* **2002**, *74*, 355. (b) Casanovas, J.; Ricart, J. M.; Rubio, J.; Illas, F.; Jimenez Mateos, J. M. *J. Am. Chem. Soc.* **1996**, *118*, 8071.

(2) Miyamoto, Y.; Cohen, M. L.; Louie, S. G. *Solid State Commun.* **1997**, *102*, 605.

(3) Liu, A. Y.; Cohen, M. L. *Science* **1989**, *245*, 841.

(4) (a) Sharma, A. K.; Ayyub, P.; Multani, M. S.; Adhi, K. P.; Ogale, S. B.; Sunderaraman, M.; Upadhyay, D. D.; Banerjee, S. *Appl. Phys. Lett.* **1996**, *69*, 3489. (b) Niu, C. M.; Lu, Y. Z.; Lieber, C. M. *Science* **1993**, *261*, 334. (c) Peng, Y. G.; Ishigaki, T.; Horiuchi, S. *Appl. Phys. Lett.* **1998**, *73*, 3671. (d) Khabashesku, V. N.; Zimmerman, J. L.; Margrave, J. L. *Chem. Mater.* **2000**, *12*, 3264. (e) Meng, X. Q.; Zhang, Z. H.; Guo, H. X.; Li, A. G.; Fan, X. J. *Solid State Commun.* **1998**, *107*, 75.

(5) Tang, C. C.; Golberg, D.; Bando, Y.; Xu, F. F.; Liu, B. D. *Chem. Commun.* **2003**, *24*, 3050.

(6) Nesting, D. C.; Badding, J. V. *Chem. Mater.* **1996**, *8*, 535.

(7) Zimmerman, J. L.; Williams, R.; Khabashesku, V. N.; Margrave, J. L. *Nano. Lett.* **2001**, *1*, 731.

(8) Guo, Q.; Xie, Y.; Wang, X.; Zhang, S.; Hou, T.; Lv, S. *Chem. Commun.* **2004**, *1*, 26.

(9) Guo, Q.; Xie, Y.; Wang, X.; Lv, S.; Hou, T.; Liu, X. *Chem. Phys. Lett.* **2003**, *380*, 84.

(10) (a) Liu, J. W.; Shao, M. W.; Tang, Q.; Zhang, S. Y.; Qian, Y. T. *J. Phys. Chem. B* **2003**, *107*, 6329. (b) O'sLoughlin, J. L.; Kiang, C.-H.; Wallace, C. H.; Reynolds, T. K.; Rao, L.; Kaner, R. B. *J. Phys. Chem. B* **2001**, *105*, 1921. (c) Wang, X. J.; Lu, J.; Xie, Y.; Du, G. A.; Guo, Q. X.; Zhang, S. Y. *J. Phys. Chem. B* **2002**, *106*, 933.

(11) Shi, L.; Gu, Y. L.; Chen, L. Y.; Yang, Z. H.; Ma, J. H.; Qian, Y. T. *Chem. Lett.* **2004**, *33*, 532.

(12) Ronning, C.; Feldermann, H.; Merk, R.; Hofsass, H. *Phys. Rev. B* **1998**, *58*, 2207.

(13) Dementjev, A. P.; de Graaf, A.; van de Sanden, M. C. M.; Maslakov, K. I.; Naumkin, A. V.; Serov, A. A. *Diamond Relat. Mater.* **2000**, *9*, 1904.

(14) Rodil, S. E.; Ferrari, A. C.; Robertson, J.; Muhl, S. *Thin Solid Films* **2002**, *420−421*, 122.

(15) Chowdhury, A. K. M. S.; Cameron, D. C.; Hashmi, M. S. J. *Thin Solid Films* **1998**, *332*, 62.

(16) Gillan, E. G. *Chem. Mater.* **2000**, *12*, 3906.

(17) Kazou, N. *Infrared and Raman Spectra of Inorganic and Coordination Compounds*; Wiley: New York, 1977.

(18) (a) Tuinstra, F.; Koenig, J. L. *J. Chem. Phys.* **1970**, *53*, 1126. (b) Mcculloch, D. C.; Prawer, S.; Hoffman, A. *Phys. Rev. B* **1994**, *50*, 5905.

(19) Kaufman, J. H.; Metin, S.; Saperstein, D. D. *Phys. Rev. B* **1989**, *39*, 13053.

(20) See supplementary Figure 1.
(21) Dillon, R. O.; Woollam, J. A.; Katkanant, V. *Phys. Rev. B* **1984**, *29*, 3482.
(22) Beeman, D.; Silverman, J.; Lynds, R.; Anderson, M. R. *Phys. Rev. B* **1984**, *30*, 870.
(23) Moreno, J. M. C.; Yoshimura, M. *J. Am. Chem. Soc.* **2001**, *123*, 741.
(24) dos Santos, M. C.; Alvarez, F. *Phys. Rev. B* **1998**, *58*, 13918.
(25) Liu, J.; Shao, M.; Tang, Q.; Chen, X.; Liu, Z.; Qian, Y. *Carbon* **2003**, *41*, 1682.
(26) Heidenreich, R. D.; Hess, W. M.; Ban, L. L. *J. Appl. Crystallogr.* **1968**, *1*, 119.
(27) Ugarte, D. *Nature* **1992**, *359*, 707.
(28) Xu, F.; Xie, Y.; Zhang, X.; Zhang, S.; Liu, X.; Tian, X. *Inorg. Chem.* **2004**, *43*, 822.
(29) Donnet, J. B. *Carbon* **1982**, *20*, 267.
(30) Xiong, Y.; Xie, Y.; Li, Z.; Wu, C.; Zhang, R. *Chem. Commun.* **2003**, *7*, 904.
(31) Vander Wal, R. L.; Tomasek, A. J.; Ticich, T. M. *Nano. Lett.* **2003**, *3*, 223.
(32) Fu, H. X.; Cao, C. B.; Zhu, H. S. *Chem. Phys. Lett.* **1999**, *314*, 223.
(33) Miller, D. R.; Wang, J.; Gillan, E. G. *J. Mater. Chem.* **2002**, *12*, 2463.